

Original Research

Identification and Characterisation of Potential Targets for N6-methyladenosine (m6A) Modification during Intervertebral Disc Degeneration

Jianlin Shen^{1,2,†}, Qiang Zhang^{2,†}, Yujian Lan³, Qingping Peng³, Ziyu Ji³, Yanjiao Wu^{4,*}, Huan Liu^{5,*} №

Academic Editor: Agnieszka Paradowska-Gorycka

Submitted: 27 June 2024 Revised: 26 August 2024 Accepted: 10 September 2024 Published: 28 November 2024

Abstract

Background: The mechanism for RNA methylation during disc degeneration is unclear. The aim of this study was to identify N6-methyladenosine (m6A) markers and therapeutic targets for the prevention and treatment of intervertebral disc degeneration (IDD). **Methods**: Methylated RNA immunoprecipitation sequencing (MeRIP-seq) and quantitative reverse transcription PCR (RT-qPCR) were employed to analyze m6A modifications of IDD-related gene expression. Bioinformatics was used to identify enriched gene pathways in IDD. m6A-RIP-qPCR was used to validate potential targets and markers. **Results and Conclusion**: Human IDD samples exhibited a distinct m6A modification pattern that allowed associated genes and pathways to be identified. These genes had functions such as "nuclear factor kappa-B (NF- κ B) binding" and "extracellular matrix components", which are crucial for IDD pathogenesis. *ANXA2* showed increased m6A modification in IDD, while *SLC3A2* and *PBX3* showed decreased m6A methylation. The results of this study offer novel insights for the prevention and treatment of IDD.

Keywords: intervertebral disc degeneration; nucleus pulposus; epigenetics; RNA methylation; N6-methyladenosine

1. Introduction

Intervertebral disc degeneration (IDD) underlies various degenerative spinal diseases, including disc herniation, spinal stenosis, and scoliosis. As the central component of intervertebral discs, the nucleus pulposus (NP) exhibits early signs of degeneration characterized by NP cell dysfunction and altered extracellular matrix (ECM) [1,2]. Mechanical stress, immune dysfunction, metabolic imbalances, and oxidative stress contribute to the development of IDD [3,4]. Effective reversal strategies for IDD are still lacking, and hence a better understanding of the molecular mechanisms that govern IDD pathogenesis is critical for improving treatment and prevention.

A key contributor to IDD pathogenesis is epigenetics, which acts as a bridge between environmental and genetic influences [5–7]. RNA methylation is a crucial epigenetic mechanism that influences post-transcriptional RNA processing through gene-level methylation, thereby impacting splicing, stability, translation, and degradation [8]. Among the different RNA modifications, N6-methyladenosine (m6A) is the most common, affecting approximately 25% of the transcriptome. m6A plays vital

roles in diverse processes including stem cell activity, cardiac hypertrophy, DNA damage response, and tumorigenesis [9,10]. There have been some reports of m6A modification during IDD and NP cell senescence. For example, expression of the m6A-modified demethylase alkylation repair homolog 5 (ALKBH5) is increased during NP cell senescence and can promote IDD through demethylationinduced NP cell senescence [11]. Also during NP cell senescence, the lncRNA NORAD can be methylated by Wilms tumor 1 associated protein (WTAP), which forms the core of the methyltransferase complex. This leads to NP cell senescence by decreasing the amount of chelated Pumilio (PUM)1/2 proteins, which subsequently increases PUM1/2-mediated degradation of the transcription factor E2F3 to further promote cellular senescence [12]. Another study showed that m6A hypomethylation of circG-PATCH2L regulates DNA damage and apoptosis through tripartite motif containing 28 (TRIM28) in IDD [13]. In addition, m6A-induced miR-143-3p promotes IDD by regulating SRY-box transcription factor 5 (SOX5) [14]. However, the functional significance and regulatory mechanisms of m6A remain largely unexplored in IDD. Despite

¹Department of Orthopaedics, Affiliated Hospital of Putian University, 351100 Putian, Fujian, China

²Central Laboratory, Affiliated Hospital of Putian University, 351100 Putian, Fujian, China

³School of Integrated Traditional Chinese and Western Medicine, Southwest Medical University, 646000 Luzhou, Sichuan, China

⁴Department of Orthopaedics, Shunde Hospital, Southern Medical University (The First People's Hospital of Shunde), 528308 Foshan, Guangdong, China

⁵Department of Orthopaedics, The Affiliated Traditional Chinese Medicine Hospital, Southwest Medical University, 646000 Luzhou, Sichuan, China

^{*}Correspondence: colt2046@163.com (Yanjiao Wu); 20016040@163.com (Huan Liu)

[†]These authors contributed equally.

the growing evidence linking m6A modification to degenerative diseases, the specific patterns and biological implications of aberrant m6A in NP tissues during IDD remain unclear.

Quercetin is a natural flavonoid found in many fruits and vegetables. It has several beneficial effects in a variety of degenerative diseases, including anti-cancer, antiinflammatory, anti-aging and antioxidant properties [15, 16]. Recent study has shown good results for quercetin in improving IDD. For example, quercetin promotes ECM homeostasis and inhibits the interleukin (IL)- 1β -induced senescence-associated secretion phenotype in NP cells. The effect of quercetin on IDD has been reported to occur through the nuclear factor erythroid 2-related factor 2 (Nrf2)/nuclear factor kappa-B (NF-κB) axis [17]. Quercetin induces autophagy in a Sirtuin 1 (SIRT1)dependent manner to protect NP cells from apoptosis and prevent oxidative stress-induced ECM degeneration, thereby attenuating IDD [18]. It was also shown to attenuate IDD by reducing p38 mitogen-activated protein kinase (p38 MAPK)-mediated autophagy [19]. In rat myeloidderived mesenchymal stem cells (MSCs), quercetin ameliorates oxidative stress-induced senescence through the miR-34a-5p/SIRT1 axis [20]. Collectively, the above studies strongly suggest that quercetin is a good candidate in the treatment of IDD. With regard to quercetin and m6A, recent study suggests that quercetin can modulate typical biochemical signalling pathways, thereby affecting epigenetic networks [21]. In hyperinsulinaemia, quercetin promotes glucose uptake, inhibits oxidative stress and ameliorates insulin resistance via m6A in mRNA for the methyltransferase-like 3 (METTL3)-mediated serinethreonine kinase protein kinase D2 (PRKD2) [22]. Although, quercetin has been linked to m6A, it is not known whether quercetin can alter IDD progression through this RNA modification. The aim of the current study was therefore to further explore the effect of quercetin on genes exhibiting differential m6A modification in IDD compared to controls.

This study explored the m6A modification profile in IDD at the whole transcriptome level. In order to characterize m6A patterns, the techniques of methylated RNA immunoprecipitation sequencing (MeRIP-seq) and RNA sequencing (RNA-seq) were applied to NP cells from IDD patients, as well as control patients who underwent lumbar spine fracture surgery. An existing gene expression profiling dataset (GSE56081) was also leveraged to identify m6A-based markers and potential therapeutic targets for IDD, with the aim of identifying novel strategies for disease prevention and treatment.

2. Materials and Methods

2.1 Patients, Specimens and Ethics Statement

NP tissues were obtained from patients undergoing lumbar spine surgery. Three IDD samples were collected

from patients with lumbar disc herniation, while three normal intervertebral discs from patients with lumbar spine fractures served as controls. All specimens were immediately stored at -80 °C until RNA isolation. This study was approved by the Ethics Committee of Shunde Hospital, Southern Medical University (No. 20200812), and all participants provided written informed consent. And all methods were performed in accordance with the relevant guidelines and regulations. The study was performed in accordance with the Declaration of Helsinki.

2.2 RNA Extraction, Quantitative PCR, and Primers

Total RNA was extracted using TRIzol reagent (15596026, Thermo Fisher Scientific, Shanghai, China). Briefly, NP tissue was directly homogenized in TRIzol. Chloroform was then added to induce phase separation, followed by centrifugation. The RNA-containing aqueous phase was isolated and precipitated with isopropanol. The RNA pellet was then washed with ethanol, air-dried, and resuspended in RNase-free water. DNase I (18047019, Thermo Fisher Scientific, Shanghai, China) treatment was performed to remove DNA contamination. Finally, RNA concentration and quality were assessed using a Nanodrop 2000 spectrophotometer (ND2000CLAPTOP, Thermo Scientific, Carlsbad, CA, USA). Isolated RNA was stored at -80 °C, or used immediately for m6A-RNA immunoprecipitation (RIP) experiments. The primer sequences used for quantitative polymerase chain reaction (qPCR) analysis are presented in Table 1.

2.3 RNA-seq and MeRIP-seq

Total RNA was extracted from IDD and normal NP tissues as described above. RNA-seq and MeRIP-seq analyses were then performed on tissue samples from individuals with IDD and normal NP to obtain transcriptome and m6A methylation profiles, respectively. The MeRIP-seq technique was carried out using previously described protocols. Briefly, the GenSeqTM m6A RNA IP kit (GS-ET-001, Cloud-Biotech Co., Ltd., Shanghai, China) was used to immunoprecipitate m6A-modified RNA, followed by library construction using the NEBNext® Ultra II Directional RNA Library Prep kit (E7760L, New England Biolabs, Ipswich, MA, USA) for both input and immunoprecipitated RNA samples. Library quality was assessed using the BioAnalyzer 2100 (G2939BA, Agilent Technologies Inc., Santa Clara, CA, USA). High-throughput sequencing was performed on the Illumina NovaSeq platform in 150 bp paired-end mode. Raw sequencing data from the NovaSeq 6000 (20012860, Illumina, San Diego, CA, USA) platform underwent image analysis, base calling, and quality control with a Q30 threshold. Adapter trimming and low-quality read filtering were performed using cutadapt software (v1.9.3, https://github.com/marcelm /cutadapt/), resulting in high-quality, clean reads. Clean reads from the input library were aligned to the reference



Table 1. RNA primer for quantitative PCR.

Gene name	Sequence 5'-3'				
FTO	Forward	GTTCACAACCTCGGTTTAGTTC			
	Reverse	CATCATCATTGTCCACATCGTC			
YTHDF3	Forward	GTTTCAGTACAAAACGGTTCGA			
	Reverse	TGGAGCATAGTAACTAGGCATG			
IGF2BP3	Forward	GAGGCGCTTTCAGGTAAAATAG			
	Reverse	AATGAGGCGGGATATTTCGTAT			
SLC3A2	Forward	CTCAACTTCTCCGACTCTACC			
	Reverse	TTCACAGTCATGTTGGCACTTA			
PBX3	Forward	CAAAGAAACATGCCCTGAACTG			
	Reverse	GCTGAGACCTGTTTTCTCTTTG			
ANXA2	Forward	ACATTGAAACAGCCATCAAGAC			
	Reverse	GAAGGCAATATCCTGTCTCTGT			
ACTB	Forward	GTGGATCAGCAAGCAGGAGT			
	Reverse	AAAGCCATGCCAATCTCATC			

Table 2. RNA primer for methylated RNA immunoprecipitation (MeRIP)-quantitative polymerase chain reaction (qPCR).

Gene name	Gene location		Sequence 5'-3'		
SLC3A2	chr9: 128697750-128697886	Forward	TCCTTGATGCCAGACGGAAA		
	CIII 9. 12809//30-12809/880	Reverse	GGGTTGCTGAGGTGTGAGTA		
PBX3	chr11: 62644255-62644351	Forward	TGGGATTACAGGCACCATGA		
		Reverse	CTGCTTCTCGGGCTCTAACT		
ANXA2	chr15: 60688601-60688626	Forward	CCCGCTTGGTTGAACACATT		
		Reverse	GGAGGAAGGAATGCAGCGTA		

genome (UCSC HG19) using STAR software (v2.7.11b, https://github.com/alexdobin/STAR). Methylated genes within each sample were first identified using MACS software (v1.4.2, https://macs3-project.github.io/MACS/), followed by analysis of differential methylation using diffReps software (v1.55.6, https://github.com/shenlab-sinai/diffreps). Peaks located on mRNA exons were retained for annotation. Finally, Gene Ontology (GO) and Pathway analyses were conducted for differentially methylated coding genes. RNA-seq and MeRIP-seq data are available in GSE260813 (https://www.ncbi.nlm.nih.gov/geo/).

2.4 MeRIP-qPCR

Briefly, total RNA was isolated from NP samples. Immunoprecipitation (IP) to enrich m6A-modified RNA fragments was then performed at 4 °C using anti-m6A antibody (202003, Synaptic Systems, Goettingen, Germany). Magnetic beads captured the antibody-RNA complexes, followed by elution of the methylated RNA to separate it from non-methylated RNA. The eluted m6A-RNA was converted to complementary DNA (cDNA) for real-time quantitative PCR (qPCR) analysis, as per the manufacturer's instructions. This allowed quantification of the m6A modification status of target genes relative to the input RNA. The primer sequences used for MeRIP-qPCR analysis are presented in Table 2.

2.5 Gene Expression Omnibus (GEO) Database and Analysis

The GSE56081 dataset encompassing gene expression profiling of mRNA from 5 normal human NP tissues and 5 degenerative NP tissues was downloaded from the National Center for Biotechnology Information (NCBI) Gene Expression Omnibus (GEO) database (https://www.ncbi.nlm.nih.gov/geo/). Differential gene expression analysis was performed using the limma package (v3.60.1, https://bioconductor.org/packages//2.7/bioc/html/limma.html).

2.6 Identification of Potential Drug Targets for the Treatment of IDD

The Herb database (http://herb.ac.cn/) was queried to identify potential binding partners for quercetin and to assess their possible therapeutic efficacy for IDD. Cytoscape software (v3.10.2, https://cytoscape.org/) was employed to construct a quercetin-target-IDD network. Network analysis was conducted to assess network properties, including degree, betweenness centrality, closeness centrality, and average shortest path length. These metrics quantify node connectivity, the influence of a node in connecting others, a node's proximity to other network members, and the average distance between nodes, respectively. Collectively, these parameters provided insights into the overall network structure.



2.7 Functional Annotation of Differentially Expressed and Methylated Genes

Differentially methylated mRNAs were subjected to functional enrichment analysis. Gene Ontology (GO, https://www.geneontology.org/) terms categorized into Molecular Function (MF), Biological Process (BP), and Cellular Component (CC) were explored to annotate gene functions and identify enriched pathways. Additionally, Kyoto Encyclopedia of Genes and Genomes (KEGG, https://www.kegg.jp/) pathway analysis was performed to further assess the involvement of these genes in specific biological processes. Significantly enriched terms and pathways were identified based on a *p*-value threshold of <0.05.

2.8 Statistical Analysis

Statistical differences between groups were assessed using the Chi-squared test or Student's *t*-test, as appropriate, on RNA sequencing and real-time quantitative PCR data. All statistical analyses were performed using Graph-Pad Prism software (v9.0, https://www.graphpad.com/scientific-software/prism/) and R software (v4.3.2, https://www.r-project.org/). Statistical significance was defined as a two-tailed *p*-value of <0.05.

3. Results

3.1 Overview of m6A-RIP Sequencing Results in IDD versus Normal NP Tissue

RNA-seq and m6A-RIP sequencing were performed to compare m6A modification patterns between NP samples from normal and IDD individuals. m6A-RIP peaks displayed significant enrichment for the expected RRACH (GGACU, UGGAG, UGCAG, AGGAG, and AGCAG), UCCUGG, UCCUGC, ACCUGG, and ACGUGG motifs, thus confirming the validity and reliability of this method (Fig. 1A). Detailed sequence quality information is provided in **Supplementary Tables 1,2**.

Over 80% of genes displayed 1–3 enriched m6A peaks in both IDD and control groups, with only 20% exceeding 4 or more peaks. The proportion of genes with one or two m6A peaks in the IDD group was lower than in the control group, while the proportion of genes with three or more m6A peaks was higher in the IDD group (Fig. 1B). This indicates consistent peak distribution across groups. However, analysis by featureCounts revealed distinct chromosomal distributions, with the IDD group showing more enriched m6A peak sequences, suggesting potentially more m6A modification in transcripts from this group (Fig. 1C). After integrating the peaks from both groups, >50% were found to be localized within coding sequences (CDS) (Fig. 1D). Both IDD and control groups showed similar enrichment (>50%) within CDS (Fig. 1E). Interestingly, LPIN3 and SLC25A38 showed a greater than 1000fold enrichment in the IDD group compared to controls. Conversely, WDR72 displayed differential m6A modification below this threshold. Table 3 lists the top 20 differentially m6A-modified mRNAs between IDD and control groups.

Further analysis compared the relative enrichment density of m6A peaks across 5' UTR, CDS, and 3' UTR regions. Compared to controls, the IDD group displayed a higher propensity for m6A modifications within the CDS region, suggesting potential alterations in the regulation of mRNA translation (Fig. 1F). Notably, the IDD group also exhibited a lower overall level of m6A modification in the 3' UTR, potentially affecting mRNA stability.

3.2 mRNAs Exhibiting Differential m6A Enrichment in Critical Signaling Pathways

To explore the biological implications of m6A modifications in IDD, Gene Ontology (GO) and KEGG pathway analyses were performed on mRNAs with identified m6A-modified peaks. mRNAs with hypermethylated peaks in the IDD group relative to controls showed significant enrichment in biological processes involving "small GTPase-mediated signal transduction" and "regulation of small GT-Pase activity", as well as in molecular functions related to "GTPase regulator activity" (Fig. 2A). Conversely, mRNAs with hypomethylated peaks in the IDD group relative to controls were strongly associated with calcium ion regulation, including processes such as "calcium ion transmembrane import into cytosol" and "regulation of calcium ion sequestering" (Fig. 2D).

KEGG pathway analysis revealed that mRNAs with hypermethylated peaks in IDD were enriched in pathways related to "transport and catabolism", "eukaryotic cellular community", and "cell motility" (Fig. 2B). This was further supported by specific pathways such as "regulation of actin cytoskeleton" and "osteoclast differentiation" (Fig. 2C). Notably, mRNAs with hypomethylated peaks in IDD showed significant association with pathways crucial for "substance dependence", "cell growth and death", and "signal transduction" (Fig. 2E), encompassing specific pathways such as "protein digestion and absorption" and "calcium signaling pathway" (Fig. 2F).

3.3 Integrated Analysis of Differential m6A Modification and Gene Expression in IDD and Control (Input) Groups

Next, sequencing data from m6A-RIP and input groups was integrated to investigate the connection between differential m6A modifications and gene expression in IDD compared to controls. A heatmap was generated to visualize gene expression profiles for the three control and three IDD samples (Fig. 3A). Differentially m6A-modified transcripts were then identified using defined criteria ($|\log$ arithm base 2 fold change (\log 2FC)|>1, p-value < 0.05). This revealed 348 genes with upregulated m6A modification and 402 genes with downregulated m6A modification levels in the IDD group relative to controls (Fig. 3B). Further analysis of the intersection between con-



Table 3. The top 20 differently methylated m6A peaks in lDD in comparison with the controls (mRNAs).

Chrom	txStart	txEnd	Gene name	Fold change	<i>p</i> -value	Regulation
chr20	39987361	39987600	LPIN3	1731.5	1.351×10^{-8}	Up
chr3	39425161	39425284	<i>SLC25A38</i>	1017.6	5.114×10^{-9}	Up
chr9	131584921	131585112	C9orf114	942.3	4.768×10^{-9}	Up
chr13	24871500	24871600	SPATA13	845.8	4.507×10^{-9}	Up
chr7	98942101	98942138	ARPC1A	782.6	4.740×10^{-9}	Up
chr19	6226987	6227000	MLLT1	769.9	3.823×10^{-9}	Up
chr5	177551601	177551920	N4BP3	691.1	4.491×10^{-9}	Up
chr22	19965480	19965560	ARVCF	629.1	3.845×10^{-9}	Up
chr1	156925501	156925591	ARHGEF11	601.4	5.971×10^{-9}	Up
chr1	209800841	209800924	LAMB3	587.0	4.345×10^{-9}	Up
chr15	53901721	53901789	WDR72	1301.9	3.866×10^{-9}	Down
chr20	35282001	35282104	NDRG3	586.7	2.461×10^{-9}	Down
chr1	55572911	55572960	USP24	527.8	3.331×10^{-9}	Down
chr1	19673621	19673860	AX748283	504.7	3.09×10^{-9}	Down
chr5	36671130	36671260	SLC1A3	465.8	5.305×10^{-9}	Down
chr17	57057781	57057980	PPM1E	446.7	3.13×10^{-9}	Down
chr5	34035751	34035860	C1QTNF3	385.4	3.167×10^{-9}	Down
chr12	7085521	7085740	LPCAT3	368.5	3.623×10^{-9}	Down
chr19	7671662	7671695	CAMSAP3	353.3	6.952×10^{-10}	Down
chr13	111992209	111992279	TEX29	344.9	2.711×10^{-9}	Down

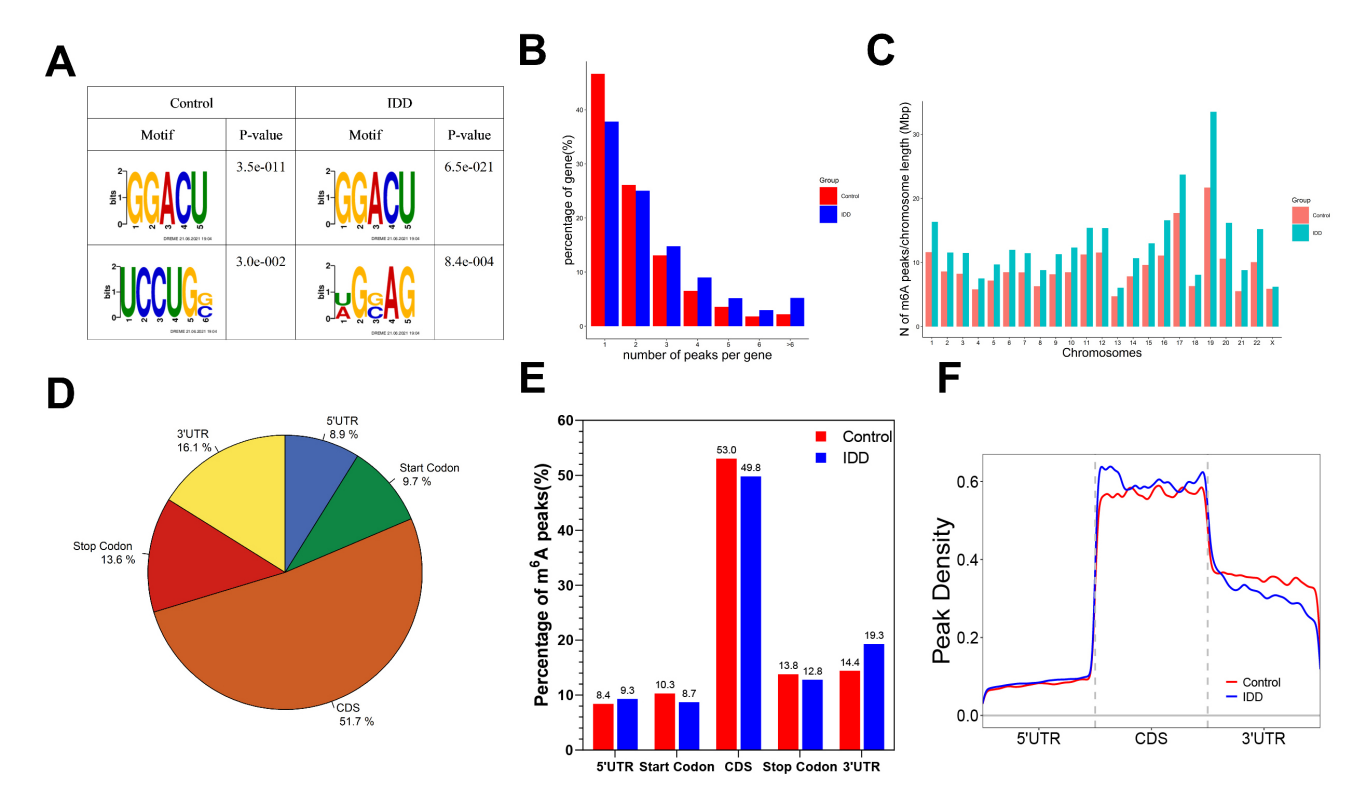


Fig. 1. Characteristics of m6A peaks within mRNAs: comparison of IDD and control NP tissues. (A) Top motifs enriched from all identified m6A peaks within mRNAs from IDD compared to control NP tissues. (B) Percentage of gene in different number peaks per gene. (C) Ratio of the number of m6A peaks to the length of the chromosome. (D) Pie diagram showing the distribution of m6A peaks in the whole transcriptome of IDD and control NP tissues. (E) Percentage of m6A peaks in different transcriptomic regions. (F) Differences in the density of m6A peaks in the indicated regions between IDD and control NP tissues. m6A, N6-methyladenosine; IDD, intervertebral disc degeneration; NP, nucleus pulposus; CDS, Coding Sequence.



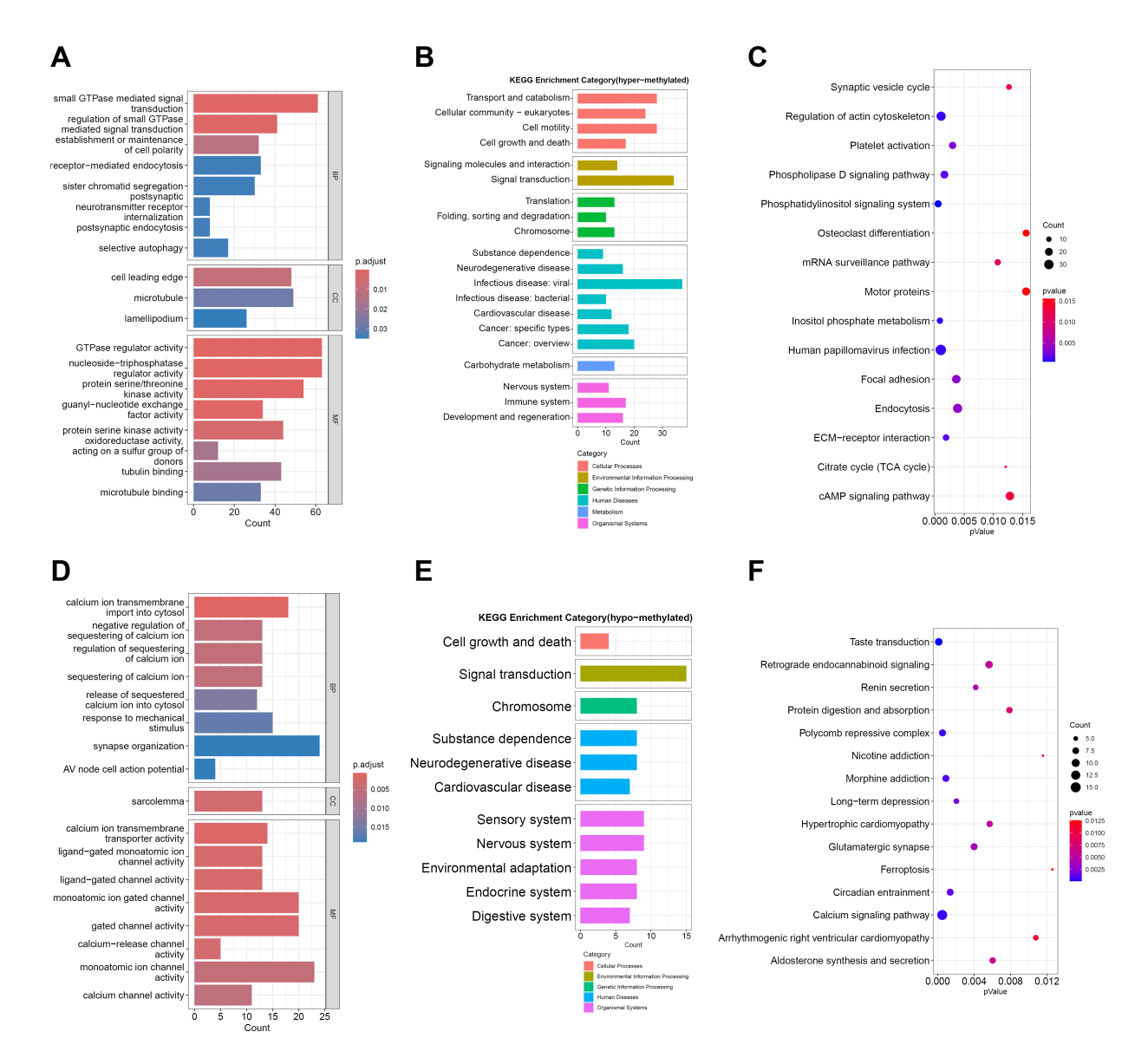


Fig. 2. Gene ontology and KEGG annotations of mRNAs with differential m6A peaks between IDD and control NP tissues. (A) GO annotation of hypermethylated genes in IDD NP tissues. (B) Subcategories of KEGG pathway enrichment of hypermethylated genes in IDD NP tissues. (C) Enrichment of hypermethylated genes in KEGG pathways. (D) GO annotation of hypomethylated genes in IDD NP tissues. (E) Subcategories of KEGG pathway enrichment of hypomethylated genes in IDD NP tissues. (F) Enrichment of hypomethylated genes in KEGG pathways. KEGG, Kyoto Encyclopedia of Genes and Genomes; GO, Gene Ontology.

trol and IDD groups identified 5327 genes that had both differential m6A modification ($|\log FC| > 1$, p-value < 0.05) and differential gene expression ($|\log FC| > 1$, p-value < 0.05). In addition, 32,139 genes were identified in the IDD group but absent in the control group, and 21,831 were identified in the control group but absent in the IDD group (Fig. 3C).

3.4 Genes with Differential m6A Modification and Differential Expression in the GEO Dataset GSE56081

To gain further insight into genes identified at the intersection between IDD and control groups, an analysis was conducted of the differential m6A modification peaks identified in the current sequencing project and the differential gene expression profile obtained from the GSE56081 dataset. In the IDD group, 134 genes were found in which m6A modification was correlated with differential gene expression. Amongst these, 63 had both increased m6A modification and increased gene expression levels, 19 had decreased m6A modification but increased gene expression levels, 12 had both decreased m6A modification and decreased gene expression levels, and 40 had increased m6A modification but decreased gene expression levels (Fig. 4A,E). The top-ranking genes based on differential fold-changes are presented in **Supplementary Table 2**.



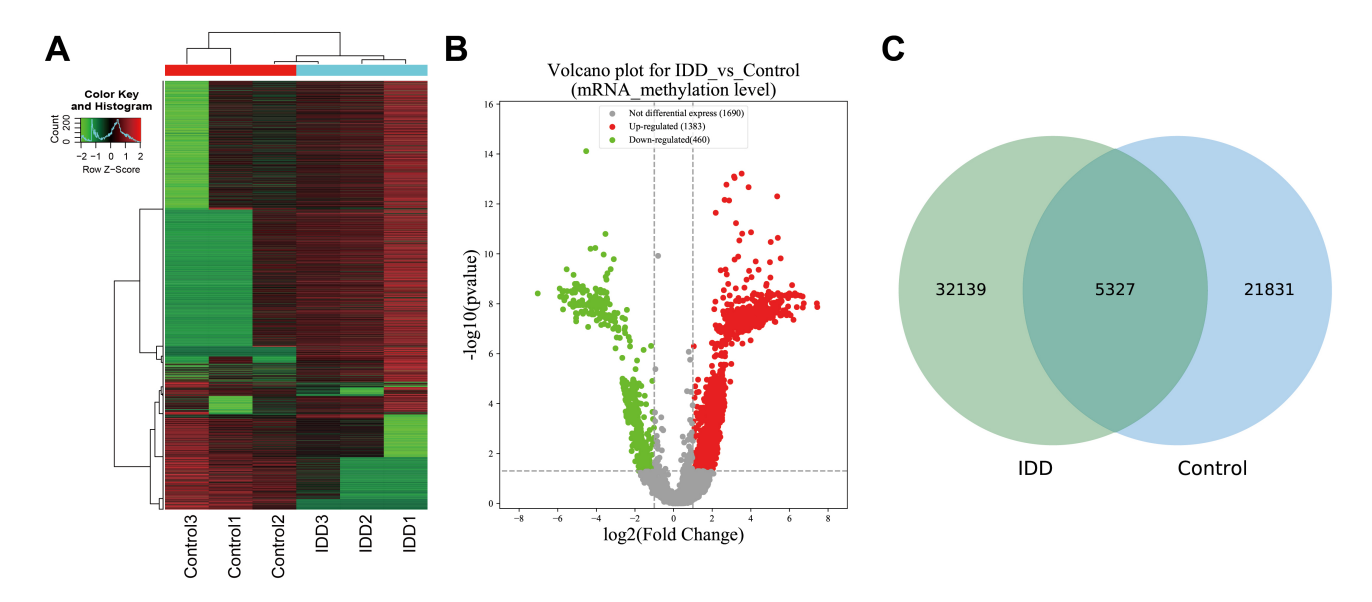


Fig. 3. Overview of gene expression in the IDD and control groups. (A) Heatmap of gene expression in the IDD and control groups. (B) Volcano plot of gene expression in the IDD and control groups (p-value < 0.05 and fold change >2). (C) Intersection of differentially expressed genes and differentially methylated genes between the IDD and control groups.

The 134 genes were subjected to GO and KEGG analysis to infer the biological functions and potential impact pathways of genes with both differential m6A modification and transcription levels between the IDD and control groups. GO enrichment analysis suggested these genes were involved in the molecular functions of "NF-kappa B binding", "ECM structural constituent", "3′,5′-cyclic-AMP phosphodiesterase activity", "collagen binding", and "response to hypoxia". They were also enriched in various cellular components, including "collagen-containing ECM" and "Golgi cisterna/stack/cisterna membrane". Additionally, they were enriched in various biological processes, including "response to hypoxia" and "regulation of mitotic cell cycle phase transition" (*p*-value < 0.05) (Fig. 4B).

KEGG results indicated the 134 genes were enriched in six categories of biological pathways. The highest proportion was observed in the "human disease" subclass, followed by "organismal systems", while "metabolism" and "genetic information processing" showed the lowest enrichment (Fig. 4C). The differential m6A modification of specific transcripts in certain pathways suggests they are potentially involved in known or inferred relevant biological phenomena associated with the experimental or computational input. Within specific signaling pathways, predominant enrichments of the 134 genes were identified in "arrhythmogenic right ventricular cardiomyopathy", "ECMreceptor interaction", "glycosaminoglycan biosynthesischondroitin sulfate/dermatan sulfate", "glycan biosynthesis and metabolism", and "circadian entrainment" (p-value < 0.05) (Fig. 4D).

3.5 Validation of Differential m6A Modification Transcripts between IDD and Control Groups by m6A-RIP-qPCR

To explore the potential mechanism of IDD treatment by quercetin, we conducted an intersection analysis between known quercetin targets and genes exhibiting differential m6A modification in IDD. The interaction network revealed six overlapping genes relevant to IDD progression: *SLC3A2*, *PBX3*, *ANXA2*, *FTO*, *YTHDF3*, and *IGF2BP3* (Fig. 5A).

RT-qPCR analysis confirmed the differential expression of these genes in the IDD group compared to the control group. *SLC3A2* was upregulated, while *PBX3* and *ANXA2* were downregulated (Fig. 5B). Interestingly, the m6A demethylase *FTO* and the m6A reader *YTHDF3* were upregulated in the IDD group, whereas the m6A reader *IGF2BP3* was downregulated (Fig. 5C), suggesting potential regulatory roles for these m6A-related proteins in IDD.

Further investigation using m6A-RIP-seq revealed differential m6A enrichment at specific sites on the *ANXA2*, *PBX3*, and *SLC3A2* transcripts. These distinct patterns were validated by m6A-RIP-qPCR, with *ANXA2* displaying increased m6A modification at chr15:60688601-60688626 in the IDD group (Fig. 6E,F). Specific regions in *SLC3A2* and *PBX3* (chr9:128697750-128697886 and chr11:62644255-62644351, respectively) showed lower levels of m6A modification in the IDD group compared to the control group (Fig. 6A–D). These findings suggest that quercetin may influence IDD progression by altering m6A modification of key genes.



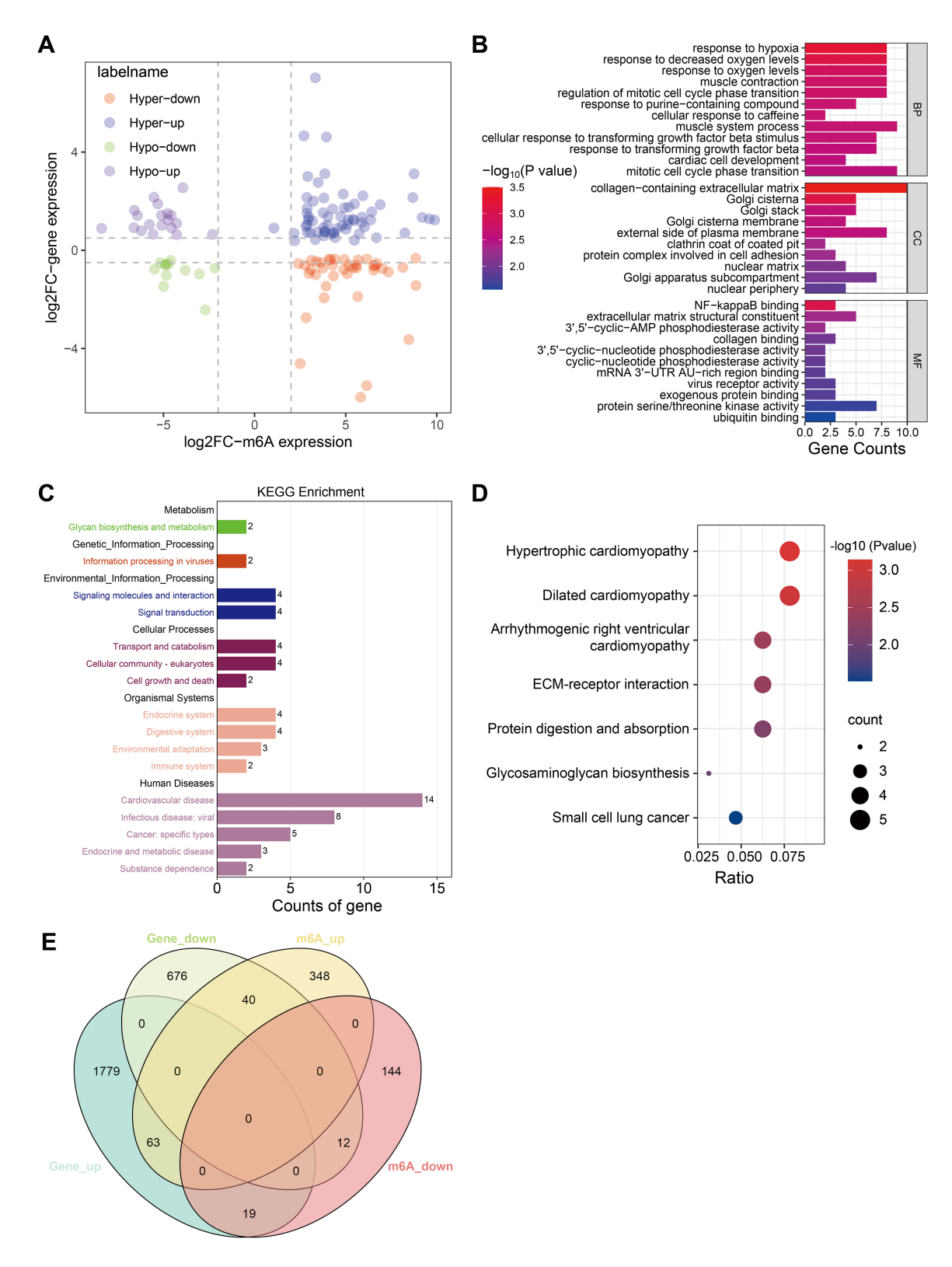


Fig. 4. Differential m6A modification and gene expression in Gene Expression Omnibus Series 56081 (GSE56081) in IDD: association with biological pathways. (A) Intersection analysis of the differential m6A modification peaks identified in this sequencing project of IDD and the differential expression profile of IDD from the GSE56081 dataset. (B) GO annotation of differentially expressed and differentially methylated genes between the IDD and control groups. (C) KEGG pathway enrichment categories for differentially methylated and differentially expressed genes between IDD and control groups. (D) KEGG enrichment analysis of differentially expressed and differentially methylated genes between IDD and control groups. (E) Venn diagram illustrating the overlap between differentially m6A-methylated genes and differentially expressed genes. ECM, extracellular matrix.

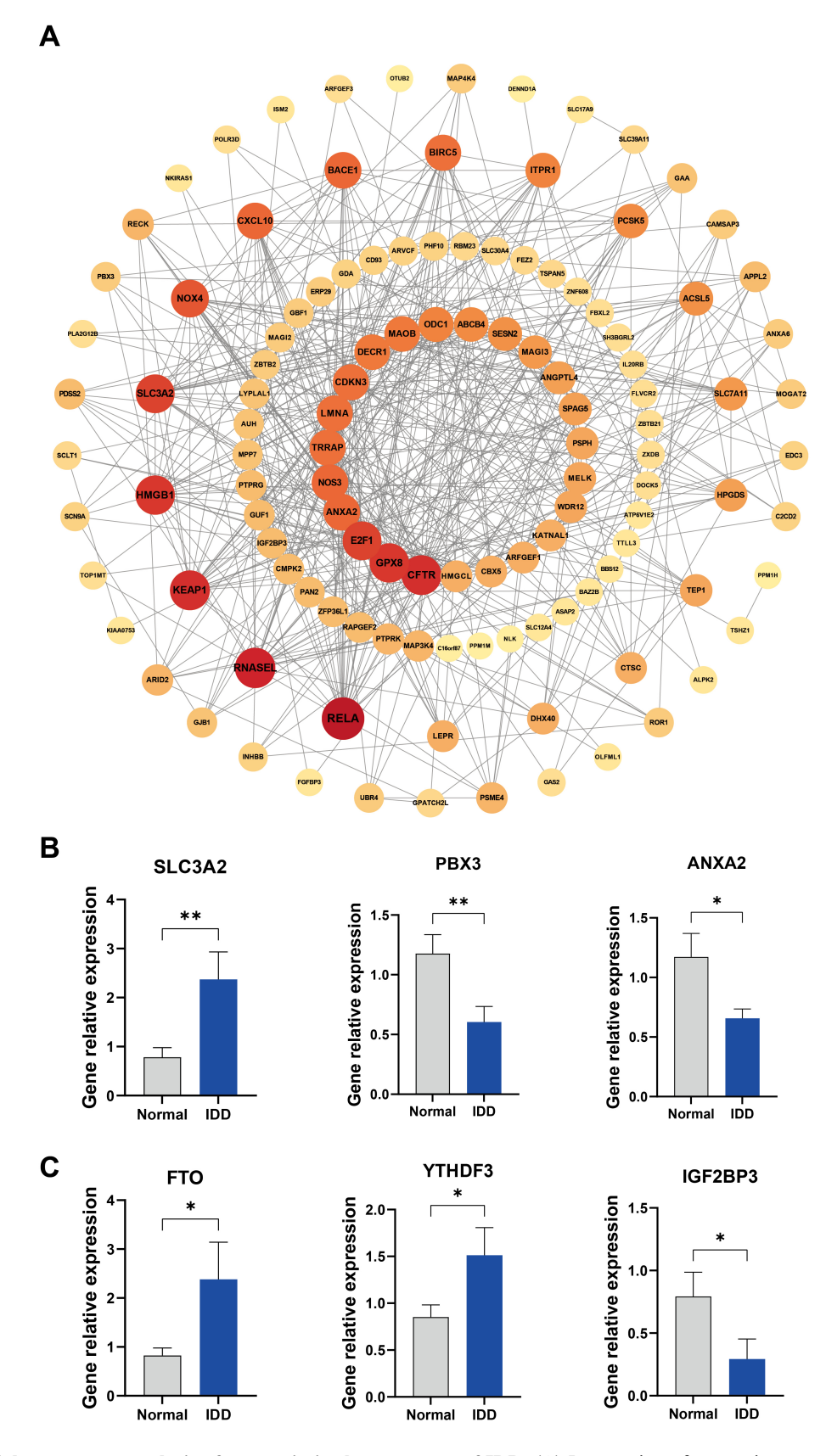


Fig. 5. Potential target gene analysis of quercetin in the treatment of IDD. (A) Intersection of quercetin targets and differentially methylated genes in IDD. (B) Real-time qPCR analysis of the expression levels of SLC3A2, PBX3, and ANXA2 in the IDD and control NP groups. (C) Real-time qPCR analysis of the expression levels of FTO, YTHDF3 and IGF2BP3 in the IDD and control NP groups. Statistical significance was defined as a two-tailed p-value, * p-value < 0.05, ** p-value < 0.01, compared with the normal group.

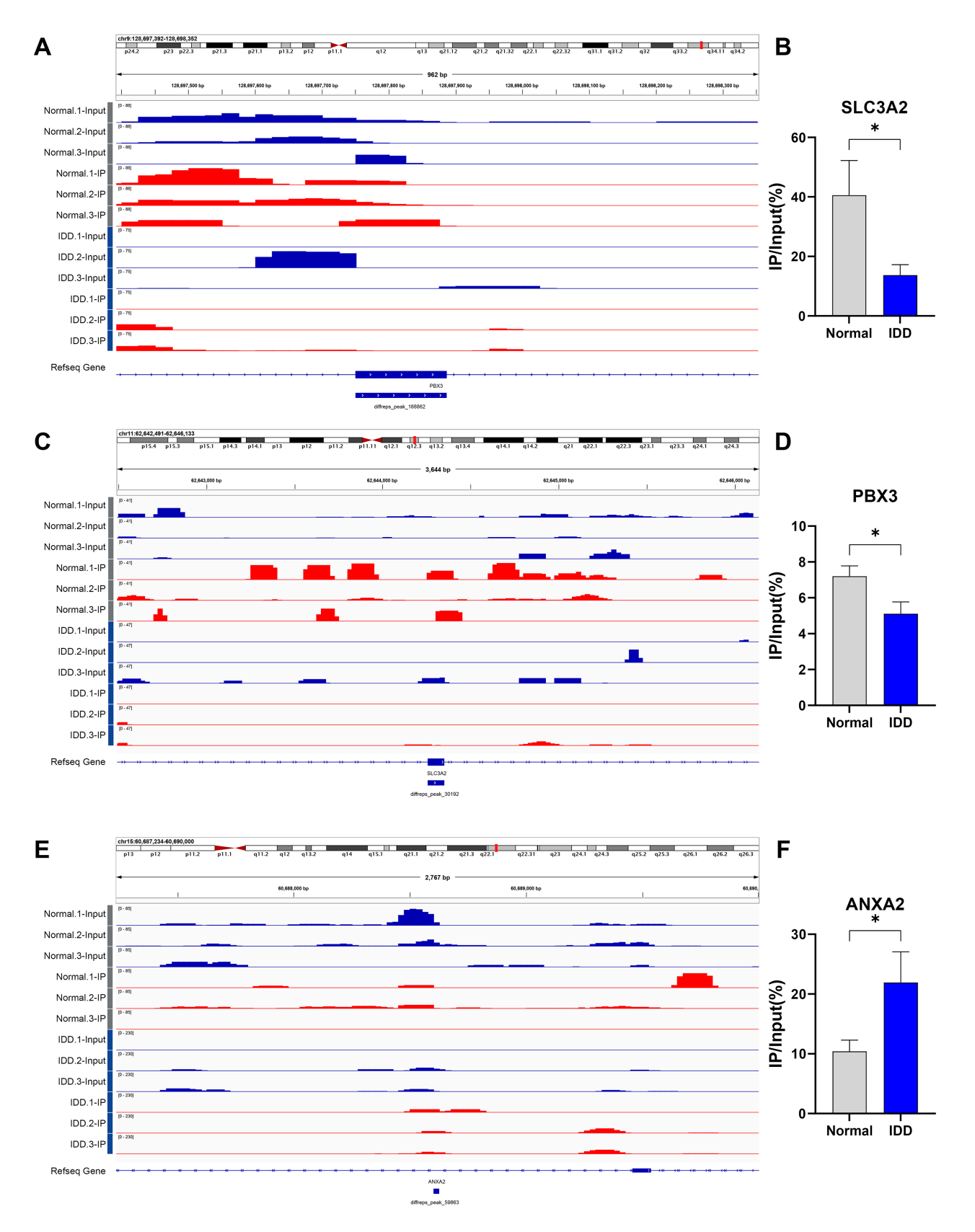


Fig. 6. Identification of differentially methylated genes between IDD and control NP tissues. (A) m6A peak map of SLC3A2 as revealed by m6A-RIP sequencing. (B) m6A-RIP qPCR results for SLC3A2 in IDD and control NP tissues. (C) m6A peak map of PBX3 as revealed by m6A-RIP sequencing. (D) m6A-RIP qPCR results for PBX3 in IDD and control NP tissues. (E) m6A peak map of ANXA2 as revealed by m6A-RIP sequencing. (F) m6A-RIP qPCR results for ANXA2 in IDD and control NP tissues. Statistical significance was defined as a two-tailed p-value, * p-value < 0.05, compared with the normal group. RIP, RNA immunoprecipitation.

4. Discussion

IDD is a complex pathological process involving multiple structural and functional changes in the spine. It is one of the main causes of various spine-related diseases, with significant impacts on patient quality of life and on the economic burden to society [23]. The complex pathogenesis of IDD involves both genetic and environmental factors, thus obscuring its precise etiology. Recent epigenetic study suggests a potential avenue to better understand the intricate pathogenesis of IDD [24]. Epigenetics is focused on the regulation of gene expression independently of the DNA sequence, and is thought to be a vital link between genetic and environmental influences [25]. A genetic study of IDD in a sample from Southern Europe examined the association between radiological disease severity of lumbar disc degeneration and specific loci. Single nucleotide polymorphisms (SNPs) in the COL1A1, COL9a3 and VDR genes were found to be associated with the progression of lumbar disc degeneration. In addition, the presence of multiple SNPs in the same individual showed a more pronounced association with disease severity. Further analysis of these genes in relation to environmental factors are needed [26]. The epigenetic modification of m6A methylation has recently attracted attention for its possible role in IDD pathogenesis. This prevalent eukaryotic mRNA modification modulates gene expression post-transcriptionally. Disruption of m6A methylation can affect RNA splicing, transportation and translation, and potentially lead to various diseases [27]. Investigation of aberrant m6A methylation in the context of IDD may lead to deeper insights into the pathogenesis of this disease and result in novel strategies for future prevention and treatment.

Several previous studies have explored the link between m6A and IDD. Zhu et al. [28] identified 30 genes with both m6A modification and altered mRNA expression in degenerated mouse medullary tissue, suggesting their potential role in m6A-driven IDD pathogenesis. Wang et al. [29] demonstrated that overexpression of FTO in rat NP tissues led to reduced m6A levels, subsequently activating the Wingless/Integrated (Wnt) signaling pathway and disrupting glucose metabolism. Gao et al. [30] reported on the molecular mechanism of WTAP/YTH N6-methyladenosine RNA binding protein 2 (YTHDF2)-mediated m6A modification in abnormal, stress-induced matrix degradation of the intervertebral disc (IVD). WTAP expression was elevated in human NP cells under tension. High WTAP expression was also detected in severely degraded human and rat NP tissues. Functionally, WTAP was shown to increase the methylation level of *TIMP3* transcripts under tension, leading to their recognition, binding and degradation by YTHDF2. Decreased *TIMP3* expression led to an increase in active matrix metalloproteinases, which ultimately induced the degradation of ECM by medullary cells. Macroscopically, this was observed to promote IDD [30]. Recently Liu et al. [31] performed MeRIP-seq to identify m6A

changes in NP tissue from rats of different ages. Similar to observations in other aged mammals such as humans, the most consistently altered motif sequence was GGACA [31]. This similarity indicates the conserved nature of m6A modification in mammals during aging [32]. Moreover, the distribution of m6A peaks occurred mainly in the CDS and 3' UTR regions. Additionally, three antisense lncRNAs were implicated in directing m6A demethylase to RNA, further highlighting the potential involvement of m6A modification in IDD.

The study to date on IDD and epigenetic modifications has mainly been focused on animals [24]. Based on the earlier finding, in the present study we conducted a comprehensive, high-throughput transcriptome analysis to explore the m6A methylome and modifier genes in IDD. We identified a large number of m6A modifications in the transcriptome of NP cells from IDD patients, suggesting they have potential roles in regulating gene expression and contributing to the disease process. Building on previous work, we also performed a comprehensive MeRIP-seq study of the m6A methylome in IDD. This analysis revealed a greater number of m6A peak sequences in the IDD group compared to the control group. Subsequent gene ontology analysis and KEGG annotation of the differential m6A peaks found in the mRNAs confirmed the impact of m6A modification on IDD. Differential m6A modification peaks were identified by sequencing, while differential expression profiles were obtained from the GSE56081 geneset. Intersection analysis revealed that m6A modification of 134 genes was associated with differential gene expression in IDD. Amongst these, 63 genes showed increased levels of both m6A modification and gene expression, 19 showed decreased levels of m6A modification and increased levels of gene expression, 12 showed decreased levels of both m6A modification and gene expression, and 40 showed increased levels of m6A modification but decreased levels of gene expression. Related enriched genes and pathways were identified by GO and KEGG analysis, respectively. Finally, our analysis found six intersections between potential target genes for quercetin and genes related to IDD progression: SLC3A2, PBX3, ANXA2, FTO, YTHDF3, and IGF2BP3. These six differential m6A-modified transcripts were validated by m6A-RIP-qPCR, resulting in identification of the SLC3A2, PBX3 and ANXA2 genes. Based on these findings, we hypothesise that m6A epigenetic modifications may be responsible for IDD, and that specific genetic modifications may further contribute to IDD.

We also investigated the potential mechanisms and biological pathways involving differentially methylated mRNAs by analyzing the distinct m6A modification patterns associated with IDD, as well as differentially expressed genes obtained through analysis of the GEO dataset GSE56081. Our findings indicate the differential genes are implicated in molecular functions including "NF- κ B binding", "structural components of the ECM", "collagen-



containing ECM", and "protein complexes involved in cell adhesion". Additionally, they are involved in biological processes including "response to hypoxia", "response to reduced oxygen levels", and "response to oxygen levels". These functions are closely linked to IDD pathogenesis and have varying impacts on the progression of this disease. Therefore, it is reasonable to infer that m6A methylation modification is a significant influencing factor in IDD.

In this study, the signalling pathways found to be related to IDD and m6A were "human disease", "organismal systems", "ECM-receptor interaction", "glycosaminoglycan biosynthesis-chondroitin sulfate/dermatan sulfate", "glycan biosynthesis and metabolism" and "circadian en-No enrichment was found for the relevant classical pathways. However, a related pathway has been studied previously. Using a smoke-exposed mouse model, cigarette smoking was reported to cause the release of mast cell (MC) restriction tetramer-like trypsin (TT) and IDD. The m6A methyltransferase-like 14 (METTL14) is involved in the release of TTs by inducing m6A methylation on 3' untranslated transcripts of the structural domain of disorganised axonemal protein (DIX), which codes for dishevelled-axin (DIX) domain-containing 1 (DIXDC1). This response increases mRNA stability and hence DIXDC1 expression. DIXDC1 interacts functionally with schizophrenia 1 interrupted cells (DISC1), thereby accelerating the degeneration and senescence of NP cells through activation of the classical Wingless/Integrated (Wnt) pathway [33]. In view of the limited number of studies on IDD and m6A-related pathways, further research is required to gain a better understanding of the mechanisms involved.

The disulfide-related gene SLC3A2 [34,35] is a member of the solute carrier family. It encodes cell-surface transmembrane proteins, including transporter proteins that regulate intracellular calcium levels and the transport of L-type amino acids [36]. In the present study, GO and KEGG enrichment analysis found that a low level of m6A in IDD was closely related to the regulation of cellular processes by calcium ions. Methylation studies on the SLC3A2 gene have mainly focused on tumours [37,38], with no reports to date on IDD. The current study is the first validation of m6A-modified SLC3A2 transcripts in IDD. Differential m6A modification was identified in specific regions of SLC3A2 at chr9:128697750-128697886, with the IDD group exhibiting decreased m6A modification compared to the control group. SLC3A2 is a known marker of ferroptosis [36,39,40], and is upregulated in the NP tissues of degenerated discs with reduced m6A levels. The m6A methylation modification therefore potentially regulates SLC3A2, thereby affecting the development of iron-dependent metaplasia in IDD. However, further investigation is required to elucidate the precise relationship and the underlying mechanisms.

PBX3 is a homologous structural domain-containing transcription factor from the pre-B-cell leukaemia family [41,42]. Research on the PBX3 gene has so far focused on cancer, including the study of histone methylation in the PBX3 promoter and enhancer regions [43,44], as well as DNA methylation. A significant increase in PBX hypomethylation was reported in acute myeloid leukaemia (AML) with core-binding factor β subunit gene (CBFB) myosin heavy chain 11 (MYH11) rearrangement [45]. This provides further evidence that PBX3 methylation plays a crucial role in disease progression. Few studies have so far been reported on the role of PBX3 in IDD. However, the present study revealed that PBX3 may be an important target for quercetin in regulating m6A methylation and thus affecting IDD. We subsequently confirmed a low level of m6A methylation in PBX3 mRNA in IDD tissues. Further studies of the possible mechanism are therefore warranted.

ANXA2 is a member of the calcium-dependent, phospholipid-binding protein family. It is involved in various cell growth and signaling pathways, especially the calcium pathway [46,47]. ANXA2 functions as an autocrine factor to promote osteoclast formation and bone resorption, as well as participating in bone remodeling [48–50]. ANXA2 also protects cells from oxidative stress [51], inhibits reactive oxygen species (ROS) production [52,53], and has a redox regulatory function. To date, much of the research on ANXA2 has focused on therapeutic resistance in cancer. Altered m6A modification of ANXA2 mRNA has also been shown to down-regulate ANXA2 expression, thus inhibiting activation of the p38 MAPK/matrix metalloproteinase-9 (MMP-9) pathway in T lymphocytes and attenuating ischemic stroke-induced neuronal damage [54]. m6A methylation of ANXA2 mRNA might therefore play an important role in disease progression. The present study found a high level of m6A methylation in ANXA2 mRNA in IDD, with concomitant low levels of ANXA2 mRNA expression. This observation suggests that changes in the ANXA2 m6A methylation level may serve as a potential target to prevent IDD disease progression.

This research has provided a comprehensive m6A modification profile for IDD, and suggests a potential role for m6A in the pathogenesis of this disease. However, our study is limited by a relatively small sample size and the absence of *in vitro* and *in vivo* functional studies. Nevertheless, our findings lay a foundation for future research that aims to develop novel therapeutic strategies for IDD, including the potential use of quercetin-based therapies.

5. Conclusion

In conclusion, we anticipate that further research in epigenetics and m6A methylation modification will lead to novel insights and pathways that may contribute to the treatment of IDD. Progress in this area should not only advance medical science and significantly benefit human health, but also offer valuable guidance for the investigation of other complex diseases.



Availability of Data and Materials

The datasets used and/or analysed during the current study are available from the corresponding author on reasonable request.

Author Contributions

JLS, QZ, YJW and HL: Conceptualization, Writing-Original Draft, Visualization, Data curation, Formal analysis. YJL, QPP, ZYJ: Conceptualization, Writing-Original Draft, Data curation, Formal analysis. JLS, HL: Writing - Review & Editing, Supervision, Funding acquisition. All authors have read and approved the final manuscript. All authors have participated sufficiently in the work and agreed to be accountable for all aspects of the work.

Ethics Approval and Consent to Participate

This study was approved by the Ethics Committee of Shunde Hospital, Southern Medical University (No. 20200812), and all patients or their families/legal guardians provided written informed consent.

Acknowledgment

We would like to thank the Department of Orthopedics, Shunde Hospital, Southern Medical University for their invaluable assistance in sample collection and preservation.

Funding

This work was supported by National Natural Science Foundation of China (82301785), key research and development projects of Sichuan Science and Technology Plan Project (2024YFFK0135) and Sichuan Province Central Guiding Local Science and Technology Development Special Project (2023ZYD0072).

Conflict of Interest

The authors declare no conflict of interest.

Supplementary Material

Supplementary material associated with this article can be found, in the online version, at https://doi.org/10.31083/j.fbl2912405.

References

- [1] Liao Z, Luo R, Li G, Song Y, Zhan S, Zhao K, *et al.* Exosomes from mesenchymal stem cells modulate endoplasmic reticulum stress to protect against nucleus pulposus cell death and ameliorate intervertebral disc degeneration in vivo. Theranostics. 2019; 9: 4084–4100.
- [2] Sun K, Jiang J, Wang Y, Sun X, Zhu J, Xu X, et al. The role of nerve fibers and their neurotransmitters in regulating intervertebral disc degeneration. Ageing Research Reviews. 2022; 81: 101733
- [3] Cheng F, Yang H, Cheng Y, Liu Y, Hai Y, Zhang Y. The role of oxidative stress in intervertebral disc cellular senescence. Frontiers in Endocrinology. 2022; 13: 1038171.
- [4] Zhang GZ, Liu MQ, Chen HW, Wu ZL, Gao YC, Ma ZJ, et al. NF-κB signalling pathways in nucleus pulposus cell function

- and intervertebral disc degeneration. Cell Proliferation. 2021; 54: e13057.
- [5] Li G, Luo R, Zhang W, He S, Wang B, Liang H, et al. m6A hypomethylation of DNMT3B regulated by ALKBH5 promotes intervertebral disc degeneration via E4F1 deficiency. Clinical and Translational Medicine. 2022; 12: e765.
- [6] Li G, Zhang W, Liang H, Yang C. Epigenetic regulation in intervertebral disc degeneration. Trends in Molecular Medicine. 2022; 28: 803–805.
- [7] Kang L, Zhang H, Jia C, Zhang R, Shen C. Epigenetic modifications of inflammation in intervertebral disc degeneration. Ageing Research Reviews. 2023; 87: 101902.
- [8] Liu Q, Gregory RI. RNAmod: an integrated system for the annotation of mRNA modifications. Nucleic Acids Research. 2019; 47: W548–W555.
- [9] An Y, Duan H. The role of m6A RNA methylation in cancer metabolism. Molecular Cancer. 2022; 21: 14.
- [10] Berulava T, Buchholz E, Elerdashvili V, Pena T, Islam MR, Lbik D, et al. Changes in m6A RNA methylation contribute to heart failure progression by modulating translation. European Journal of Heart Failure. 2020; 22: 54–66.
- [11] Lei Y, Zhan E, Chen C, Hu Y, Lv Z, He Q, et al. ALKBH5-mediated m6A demethylation of Runx2 mRNA promotes extracellular matrix degradation and intervertebral disc degeneration. Cell Bioscience. 2024; 14: 79.
- [12] Li G, Ma L, He S, Luo R, Wang B, Zhang W, et al. WTAP-mediated m⁶A modification of lncRNA NORAD promotes intervertebral disc degeneration. Nature Communications. 2022; 13: 1469.
- [13] Chen Z, Song J, Xie L, Xu G, Zheng C, Xia X, et al. N6-methyladenosine hypomethylation of circGPATCH2L regulates DNA damage and apoptosis through TRIM28 in intervertebral disc degeneration. Cell Death and Differentiation. 2023; 30: 1957–1972.
- [14] Gao D, Hu B, Ding B, Zhao Q, Zhang Y, Xiao L. N6-Methyladenosine-induced miR-143-3p promotes intervertebral disc degeneration by regulating SOX5. Bone. 2022; 163: 116503.
- [15] de Oliveira MR, Nabavi SM, Braidy N, Setzer WN, Ahmed T, Nabavi SF. Quercetin and the mitochondria: A mechanistic view. Biotechnology Advances. 2016; 34: 532–549.
- [16] He Y, Cao X, Guo P, Li X, Shang H, Liu J, et al. Quercetin induces autophagy via FOXO1-dependent pathways and autophagy suppression enhances quercetin-induced apoptosis in PASMCs in hypoxia. Free Radical Biology & Medicine. 2017; 103: 165–176.
- [17] Shao Z, Wang B, Shi Y, Xie C, Huang C, Chen B, *et al.* Senolytic agent Quercetin ameliorates intervertebral disc degeneration via the Nrf2/NF-κB axis. Osteoarthritis and Cartilage. 2021; 29: 413–422.
- [18] Wang D, He X, Wang D, Peng P, Xu X, Gao B, *et al.* Quercetin Suppresses Apoptosis and Attenuates Intervertebral Disc Degeneration via the SIRT1-Autophagy Pathway. Frontiers in Cell and Developmental Biology. 2020; 8: 613006.
- [19] Zhang S, Liang W, Abulizi Y, Xu T, Cao R, Xun C, *et al.* Quercetin Alleviates Intervertebral Disc Degeneration by Modulating p38 MAPK-Mediated Autophagy. BioMed Research International. 2021; 2021: 6631562.
- [20] Zhao WJ, Liu X, Hu M, Zhang Y, Shi PZ, Wang JW, et al. Quercetin ameliorates oxidative stress-induced senescence in rat nucleus pulposus-derived mesenchymal stem cells via the miR-34a-5p/SIRT1 axis. World Journal of Stem Cells. 2023; 15: 842– 865.
- [21] Zhu J, Cheng X, Naumovski N, Hu L, Wang K. Epigenetic regulation by quercetin: a comprehensive review focused on its biological mechanisms. Critical Reviews in Food Science and Nutrition. 2023; 1–20.



- [22] Jiao Y, Williams A, Wei N. Quercetin ameliorated insulin resistance via regulating METTL3-mediated N6-methyladenosine modification of PRKD2 mRNA in skeletal muscle and C2C12 myocyte cell line. Nutrition, Metabolism, and Cardiovascular Diseases: NMCD. 2022; 32: 2655–2668.
- [23] Liu W, Ma Z, Wang Y, Yang J. Multiple nano-drug delivery systems for intervertebral disc degeneration: Current status and future perspectives. Bioactive Materials. 2022; 23: 274–299.
- [24] Kang L, Zhang H, Jia C, Zhang R, Shen C. Epigenetic modifications of inflammation in intervertebral disc degeneration. Ageing Research Reviews. 2023; 87: 101902.
- [25] Bagot RC, Meaney MJ. Epigenetics and the biological basis of gene x environment interactions. Journal of the American Academy of Child and Adolescent Psychiatry. 2010; 49: 752– 771.
- [26] Toktaş ZO, Ekşi MŞ, Yılmaz B, Demir MK, Özgen S, Kılıç T, et al. Association of collagen I, IX and vitamin D receptor gene polymorphisms with radiological severity of intervertebral disc degeneration in Southern European Ancestor. European Spine Journal. 2015; 24: 2432–2441.
- [27] Erson-Bensan AE, Begik O. m6A Modification and Implications for microRNAs. MicroRNA. 2017; 6: 97–101.
- [28] Zhu B, Chen HX, Li S, Tan JH, Xie Y, Zou MX, *et al.* Comprehensive analysis of N6-methyladenosine (m⁶A) modification during the degeneration of lumbar intervertebral disc in mice. Journal of Orthopaedic Translation. 2021; 31: 126–138.
- [29] Wang X, Chen N, Du Z, Ling Z, Zhang P, Yang J, et al. Bioinformatics analysis integrating metabolomics of m⁶A RNA microarray in intervertebral disc degeneration. Epigenomics. 2020; 12: 1419–1441.
- [30] Gao D, Zhao Q, Liu C, Zhang Y, Xiao L. Abnormal stress promotes intervertebral disc degeneration through WTAP/YTHDF2-dependent TIMP3 m6A modification. Journal of Cellular Physiology. 2024; 239: e31219.
- [31] Liu L, Sun H, Zhang Y, Liu C, Zhuang Y, Liu M, et al. Dynamics of N6-methyladenosine modification during aging and their potential roles in the degeneration of intervertebral disc. JOR Spine. 2024; 7: e1316.
- [32] Shafik AM, Zhang F, Guo Z, Dai Q, Pajdzik K, Li Y, et al. N6-methyladenosine dynamics in neurodevelopment and aging, and its potential role in Alzheimer's disease. Genome Biology. 2021; 22: 17.
- [33] Tu J, Li W, Hansbro PM, Yan Q, Bai X, Donovan C, et al. Smoking and tetramer tryptase accelerate intervertebral disc degeneration by inducing METTL14-mediated DIXDC1 m⁶ modification. Molecular Therapy: the Journal of the American Society of Gene Therapy. 2023; 31: 2524–2542.
- [34] Zhang Y, Sun J, Li M, Hou L, Wang Z, Dong H, *et al.* Identification and validation of a disulfidptosis-related genes prognostic signature in lung adenocarcinoma. Heliyon. 2023; 10: e23502.
- [35] Jiang C, Xiao Y, Xu D, Huili Y, Nie S, Li H, *et al.* Prognosis Prediction of Disulfidptosis-Related Genes in Bladder Cancer and a Comprehensive Analysis of Immunotherapy. Critical Reviews in Eukaryotic Gene Expression. 2023; 33: 73–86.
- [36] Zhang D, Wu X, Xue X, Li W, Zhou P, Lv Z, *et al.* Ancient dormant virus remnant ERVW-1 drives ferroptosis via degradation of GPX4 and SLC3A2 in schizophrenia. Virologica Sinica. 2024; 39: 31–43.
- [37] Chen Z, Li R, Fang M, Wang Y, Bi A, Yang L, *et al.* Integrated analysis of FKBP1A/SLC3A2 axis in everolimus inducing ferroptosis of breast cancer and anti-proliferation of T lymphocyte. International Journal of Medical Sciences. 2023; 20: 1060–1078.
- [38] Wang F, Sun Z, Zhang Q, Yang H, Yang G, Yang Q, et al. Curdione induces ferroptosis mediated by m6A methylation via METTL14 and YTHDF2 in colorectal cancer. Chinese

- Medicine. 2023; 18: 122.
- [39] Xiang P, Chen Q, Chen L, Lei J, Yuan Z, Hu H, et al. Metabolite Neu5Ac triggers SLC3A2 degradation promoting vascular endothelial ferroptosis and aggravates atherosclerosis progression in ApoE^{-/-}mice. Theranostics. 2023; 13: 4993–5016.
- [40] Xiong H, Zhai Y, Meng Y, Wu Z, Qiu A, Cai Y, et al. Acidosis activates breast cancer ferroptosis through ZFAND5/SLC3A2 signaling axis and elicits M1 macrophage polarization. Cancer Letters. 2024; 587: 216732.
- [41] Morgan R, Pandha HS. PBX3 in Cancer. Cancers. 2020; 12: 431.
- [42] Luo X, Wei M, Li W, Zhao H, Kasim V, Wu S. PBX3 promotes pentose phosphate pathway and colorectal cancer progression by enhancing G6PD expression. International Journal of Biological Sciences. 2023; 19: 4525–4538.
- [43] Sun H, Huang H, Li D, Zhang L, Zhang Y, Xu J, *et al.* PBX3 hypermethylation in peripheral blood leukocytes predicts better prognosis in colorectal cancer: A propensity score analysis. Cancer Medicine. 2019; 8: 4001–4011.
- [44] Zhang W, Zhao C, Zhao J, Zhu Y, Weng X, Chen Q, et al. Inactivation of PBX3 and HOXA9 by down-regulating H3K79 methylation represses NPM1-mutated leukemic cell survival. Theranostics, 2018; 8: 4359–4371.
- [45] Hájková H, Fritz MHY, Haškovec C, Schwarz J, Šálek C, Marková J, et al. CBFB-MYH11 hypomethylation signature and PBX3 differential methylation revealed by targeted bisulfite sequencing in patients with acute myeloid leukemia. Journal of Hematology & Oncology. 2014; 7: 66.
- [46] Ninomiya K, Ohta K, Kawasaki U, Chiba S, Inoue T, Kuranaga E, *et al.* Calcium influx promotes PLEKHG4B localization to cell-cell junctions and regulates the integrity of junctional actin filaments. Molecular Biology of the Cell. 2024; 35: ar24.
- [47] Zhang H, Dong X, Ding X, Liu G, Yang F, Song Q, et al. Bufalin targeting CAMKK2 inhibits the occurrence and development of intrahepatic cholangiocarcinoma through Wnt/β-catenin signal pathway. Journal of Translational Medicine. 2023; 21: 900.
- [48] Klabklai P, Phetfong J, Tangporncharoen R, Isarankura-Na-Ayudhya C, Tawonsawatruk T, Supokawej A. Annexin A2 Improves the Osteogenic Differentiation of Mesenchymal Stem Cells Exposed to High-Glucose Conditions through Lessening the Senescence. International Journal of Molecular Sciences. 2022; 23: 12521.
- [49] Chen G, Huang G, Lin H, Wu X, Tan X, Chen Z. MicroRNA-425-5p modulates osteoporosis by targeting annexin A2. Immunity & Ageing: i & a. 2021: 18: 45.
- [50] Zhou X, Wu LF, Wang WY, Lu X, Jiang ZH, Zhang YH, et al. Anxa2 attenuates osteoblast growth and is associated with hip BMD and osteoporotic fracture in Chinese elderly. PloS One. 2018; 13: e0194781.
- [51] Madureira PA, Hill R, Miller VA, Giacomantonio C, Lee PWK, Waisman DM. Annexin A2 is a novel cellular redox regulatory protein involved in tumorigenesis. Oncotarget. 2011; 2: 1075– 1093.
- [52] He S, Li X, Li R, Fang L, Sun L, Wang Y, et al. Annexin A2 Modulates ROS and Impacts Inflammatory Response via IL-17 Signaling in Polymicrobial Sepsis Mice. PLoS Pathogens. 2016; 12: e1005743.
- [53] Ito S, Kuromiya K, Sekai M, Sako H, Sai K, Morikawa R, et al. Accumulation of annexin A2 and S100A10 prevents apoptosis of apically delaminated, transformed epithelial cells. Proceedings of the National Academy of Sciences of the United States of America. 2023; 120: e2307118120.
- [54] Liu B, Xing Z, Song F, Li D, Zhao B, Xu C, et al. METTL3-mediated ANXA2 inhibition confers neuroprotection in ischemic stroke: Evidence from in vivo and in vitro studies. FASEB Journal: Official Publication of the Federation of American Societies for Experimental Biology. 2023; 37: e22974.

